

Enhanced ferromagnetism and magnetoelectric response in quenched $BiFeO_3$-based ceramics

Qi Pan(潘祺), Bao-Jin Chu(初宝进)

Citation: Chin. Phys. B . 2020, 29(8): 087501 . **doi:** 10.1088/1674-1056/ab9736
Journal homepage: http://cpb.iphy.ac.cn; http://iopscience.iop.org/cpb

What follows is a list of articles you may be interested in

Dynamical anisotropic magnetoelectric effects at ferroelectric/ferromagnetic insulator interfaces

Yaojin Li(李耀进), Vladimir Koval, Chenglong Jia(贾成龙)
Chin. Phys. B . 2019, 28(9): 097501 . **doi:** 10.1088/1674-1056/ab37f7

Voltage control of ferromagnetic resonance and spin waves

Xinger Zhao(赵星儿), Zhongqiang Hu(胡忠强), Qu Yang(杨曲), Bin Peng(彭斌), Ziyao Zhou(周子尧), Ming Liu(刘明)
Chin. Phys. B . 2018, 27(9): 097505 . **doi:** 10.1088/1674-1056/27/9/097505

Multiferroic and enhanced microwave absorption induced by complex oxide interfaces

Cuimei Cao(曹翠梅), Chunhui Dong(董春晖), Jinli Yao(幺金丽), Changjun Jiang(蒋长军)
Chin. Phys. B . 2018, 27(1): 017503 . **doi:** 10.1088/1674-1056/27/1/017503

Nonvolatile control of transport and magnetic properties in magnetoelectric heterostructures by electric field

Qian Li(李潜), Dun-Hui Wang(王敦辉), Qing-Qi Cao(曹庆琪), You-Wei Du(都有为)
Chin. Phys. B . 2017, 26(9): 097502 . **doi:** 10.1088/1674-1056/26/9/097502

Theoretical study of mutual control mechanism between magnetization and polarization in multiferroic materials

Liu Yu, Zhai Liang-Jun, Wang Huai-Yu
Chin. Phys. B . 2015, 24(3): 037510 . **doi:** 10.1088/1674-1056/24/3/037510

Enhanced ferromagnetism and magnetoelectric response in quenched $BiFeO_3$-based ceramics*

Qi Pan(潘祺) and Bao-Jin Chu(初宝进)†

Key Laboratory of Materials for Energy Conversion, Chinese Academy of Sciences (CAS), Department of Materials Science and Engineering, University of Science and Technology of China, Hefei 230026, China

(Received 28 March 2020; revised manuscript received 24 May 2020; accepted manuscript online 28 May 2020)

The piezoelectric, ferromagnetism, and magnetoelectric response of $BiFeO_3$–$BaTiO_3$ ceramics with the compositions around the morphotropic phase boundary (MPB) of the solid solution are systematically investigated after the ceramics have been quenched from a high temperature. We find that the ferromagnetism of the quenched ceramics is greatly enhanced. An enhanced piezoelectric response d_{33} larger than 200 pC/N, which could be sustained up to 350 °C, is measured. As a result of enhanced ferromagnetism and piezoelectric response, a large magnetoelectric response $\sim$ 1.3 V/cm·Oe (1 Oe = 79.5775 A·m^{-1}) is obtained near the mechanical resonance frequency of the quenched ceramic samples. Our research also shows that in addition to the ferromagnetism and piezoelectric response, the mechanical quality factor is another important parameter to achieve high magnetoelectric response because the physical effects are coupled through mechanical interaction in $BiFeO_3$-based materials. Our work suggests that quenching is an effective approach to enhancing the magnetoelectric response of $BiFeO_3$-based materials and the materials belong to single-phase multiferroic materials with high magnetoelectric response.

Keywords: multiferroic materials, magnetoelectric, ferromagnetic, piezoelectric

PACS: 75.85.+t, 76.50.+g, 77.55.H– **DOI:** 10.1088/1674-1056/ab9736

1. Introduction

Multiferroic materials, in which ferroelectric orders coexist with ferromagnetic (or antiferromagnetic) orders, have been brought into focus due to their potential applications in sensors, transducers, and memories.[1,2] Different types of multiferroic materials have been studied in recent years, but many of the materials are not desirable for practical applications because the ferroelectric or ferromagnetic (or antiferromagnetic) order is often found at a temperature much below room temperature.[3–6] The $BiFeO_3$ (BFO) is one of the rare cases of multiferroic materials with both high Curie temperature T_c ($\sim$ 825 °C, for ferroelectric order)[7] and high Néel temperature ($\sim$ 370 °C, for the antiferromagnetic order).[8] However, BFO ceramics or thin film often exhibits large leakage, which affects the switching of ferroelectric polarization and the relevant functional properties, such as piezoelectric response.[9] In addition, although BFO possesses strong ferroelectricity, it is an antiferromagnetic (or weakly ferromagnetic) material.[10] Furthermore, the ferroelectric and antiferromagnetic (or ferromagnetic) orders in BFO originate from different microscopic mechanisms.[11] Due to these reasons, the magnetoelectric coupling effect of BFO is normally weak. Doping with aliovalent or isovalent ions, or forming solid solution with other ferroelectric compounds is an effective way to reduce the leakage and improve the ferroelectric or magnetic properties of BFO.[12–15] The solid solution of BFO and $BaTiO_3$ (BTO) is a typical material system, which has been intensively investigated. The solid solution of BFO with the appropriate amount of BTO was found to exhibit reduced conductivity, and enhanced ferroelectric or magnetic properties.[16] For example, it was found that the dielectric, ferroelectric and magnetoelctric properties were enhanced in BFO–BTO ceramics compared with BFO ceramics. It was also reported that Gd and $Bi(Zn_{0.5}\ Ti_{0.5})O_3$-modified BFO–BTO ceramics exhibited improved ferroelectricitcy.[17–19] The BFO and BTO have rhombohedral and tetragonal structures, respectively, and are similar to the observations in $Pb(Zr,Ti)O_3$ (PZT) solid solution.[20] A morphotropic phase boundary (MPB) emerges in the BFO–BTO solid solution. For the compositions near MPB, some physical properties of BFO–BTO ceramics, such as piezoelectric response, reach the maximum extents.[21] Due to this reason, the BFO–BTO ceramics has also been studied as high-T_c lead-free piezoelectrics. In addition to the modification of compositions via doping or solid solution approach, processing has a significant effect on the physical properties of the BFO-based materials. Quenching the sintered BFO-based ceramics from a high temperature was found to reduce the conductivity and improve the ferroelectricity.[22,23]

The magnetoelectric (ME) response is the generation of electric polarization P (or magnetization M) upon applying a

*Project supported by the National Natural Science Foundation of China (Grant Nos. 51672261 and 51373161) and the National Key Research and Development Program of China (Grant No. 2017YFA0701301).

†Corresponding author. E-mail: chubj@ustc.edu.cn

© 2020 Chinese Physical Society and IOP Publishing Ltd

magnetic field H (or electric field E).[24–27] Like many multiferroic materials, the BFO-based materials have a weak ME response. An enhanced ME response at room temperature compared with BFO has been observed in BFO–BTO solid solution because of the improved ferroelectricity and ferromagnetism. The measured ME response in BFO–BTO thin film is typically around 0.1 V/cm·Oe.[28] Further doping of BFO–BTO ceramics can improve the ME response. For example, $LaFeO_3$ and $La(Co_{0.5}Mn_{0.5})O_3$ modification of BFO–BTO ceramics enhances the ME response to ~ 0.67 V/cm·Oe.[29,30] However, the ME response of BFO-based materials is still much weaker than that measured in magnetoelectric composites fabricated by magnetostrictive and piezoelectric materials, and the ME response of many composites can often be higher than 1 V/cm·Oe.[31–33]

Although the effect of quenching on the ferroelectric and piezoelectric properties of BFO-based materials are frequently studied, its effect on the ferromagnetism and ME response has seldom been reported. In this work, the piezoelectric response, ferromagnetism, and ME response of the quenched BFO–BTO ceramics with compositions near MPB are systematically investigated. We show that the quenching process not only improves the piezoelectric response, but also enhances ferromagnetism and ME response. A large ME response > 1 V/cm·Oe is achieved in the BFO–BTO ceramics at mechanical resonance frequency. We also find that the highest ME response is not measured in compositions with the highest piezoelectric response nor with the strongest ferromagnetism. We propose that the mechanical quality factor should play an important role in generating the high ME response in BFO–BTO ceramics.

2. Experimental procedure

The $(1-x)BiFeO_3$–$xBaTiO_3$ ($(1-x)$BFO–xBTO) ceramic samples with the compositions in a range from $x = 0.25$ to $x = 0.4$ were prepared by using the conventional solid-state reaction method. The Bi_2O_3 (purity 99.9%), $BaCO_3$ (purity 99.9%), Fe_2O_3 (purity 99.9%), TiO_2 (purity 98.0%) were used as starting materials. All the raw materials are weighed according to stoichiometric ratio of the ceramics. Alcohol was added into the raw materials followed by ball milling. The mixture was calcined at 850 °C for 1 h and then at 940 °C for 1 h in sequence. The powder was pressed into disk samples by using polyvinyl alcohol as a binder. The wafers were heated at 600 °C for 3 h to remove the binder and then sintered at 1000 °C–1030 °C for 20 h. The sintered samples were abraded to a thickness of 0.4 mm by using sand paper. The abraded samples were treated at 850 °C for 30 min and then quickly quenched in the air. After being quenched, the ceramic wafers were cut into ceramic bars with the size of 20 mm×3 mm×0.4 mm by using a wire cutting machine (STX-202A, Kejing auto-instrument Co., Ltd., Shenyang). The crystal structures of $(1-x)$BFO–xBTO ceramics were measured by x-ray diffraction (XRD) through using Rigaku Smartlab diffractometer (Rigaku, Tokyo, Japan) The microstructure for each of the ceramic samples was examined by using a scanning electron microscope (SEM, Sirion200, FEI, USA).

Gold electrodes were deposited on the samples for electrical tests by using a sputter coater (EMS150T, Electron Microscopy Sciences, Hatfield, PA, USA). A quasi-static d_{33} meter (ZJ-6A, Institute of Acoustics, CAS, Beijing, China) was used to measure the piezoelectric coefficient d_{33} for each of the poled $(1-x)$BFO–xBTO samples. The poling process was performed at an electric field of 5 kV/mm at 120 °C for 15 min. The dielectric properties of $(1-x)$BFO–xBTO ceramics were measured by an LCR meter (model E4980, Agilent Technology, Santa Clara, CA, USA). The polarization–electric field (P–E) hysteresis loops were measured by using a modified Sawyer–Tower circuit (Polyktech, State College, USA). The vibrating sample magnetometer (SQUID-VSM, Quantum design, USA) was used to measure the magnetic hysteresis loops of $(1-x)$BFO–xBTO samples. The ME response was determined by a commercial ME measurement system (Super ME, Quantum design, USA). The magnetoelectric response of the BFO–BTO ceramics was measured by using the same procedure as that in Refs. [34,35]. During the measurement, a direct current (DC) magnetic field was applied to the ceramic samples. At the same time, a small AC magnetic field (< 2 Oe) was applied to the samples to attain the magnetoelectric coefficient at this specific DC field. The DC magnetic field can be varied to obtain the coefficients under different DC fields. The impedance spectra of the poled $(1-x)$BFO–xBTO ceramic samples were measured by an impedance analyzer (4294A, Agilent, Santa Clara, CA) and the mechanical quality factor was obtained from the impedance spectra.[36]

3. Results and discussion

Figure 1(a) shows the XRD patterns of $(1-x)$BFO–xBTO ceramic samples with x in a range from 0.25 to 0.4. All the compositions have a perovskite structure without impurity phase according to the XRD patterns.[22] For BFO-based materials, (110) and (111) pseudocubic peaks have often been used to identify the phase structure, and in Fig. 1(a), the peaks are also shown.[37–39] The splitting of both (110) and (111) peaks, which indicates a rhombohedral (R) phase,[37] is observed in 0.75BFO–0.25BTO ceramics. A further increase in BTO content leads the crystal structure to transform from rhombohedral phase to pseudo-cubic phase. The 0.7BFO–0.3BTO ceramic has a structure with the features of both

rhombohedral phase and pseudocubic phase, and the composition is thought to be near the rhombohedral–pseudo cubic (R–C) phase boundary. Figure 1(b) shows the cross-sectional SEM images of the $(1-x)$BFO–xBTO ceramic samples. All the compositions exhibit a dense microstructure and the ceramic grains have a well-defined shape. The grain size of the ceramics is in a range of 5 μm–10 μm.

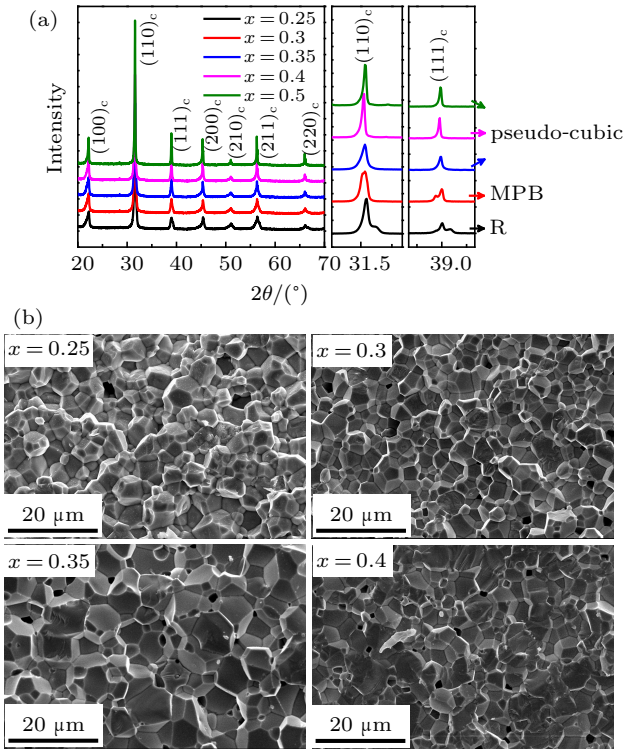


Fig. 1. (a) XRD patterns of $(1-x)$BFO–xBTO ceramic samples ($x = 0.25$–0.4), with two panels on the right showing (110) and (111) pseudo-cubic peaks, and (b) cross-sectional SEM images of $(1-x)$BFO–xBTO ceramic samples.

Figure 2(a) shows the temperature dependence of the weak-field dielectric constant and loss of $(1-x)$BFO–xBTO ceramic samples. The dielectric maximum temperature (T_m) can be regarded as the Curie temperature of the material. Consistent with prior studies, T_m gradually moves to a lower temperature with the increase of BTO content, indicating the lowering of Curie temperature of the solid solution with more BTO content in the composition.[21,40] The dielectric loss of BFO–BTO ceramics is in a range from 0.07 to 0.14 below 300 °C. At a high temperature, the dielectric loss increases dramatically as a result of a high conduction or the contribution from other polarization mechanisms. The *P*–*E* hysteresis loops of BFO–BTO ceramics are shown in Fig. 2(b). With the amount of BTO increasing, the coercive field of the ceramics decreases as shown in the inset of Fig. 2(b). When x is increased to 0.4, the ceramic exhibits a slim *P*–*E* loop. It implies that the ferroelectricity is de-stabilized by the incorporation of BTO into the materials, and this result is consistent with the conclusion from XRD that the structure of the BFO–BTO ceramics changes towards pseudocubic structure with BTO content increasing.

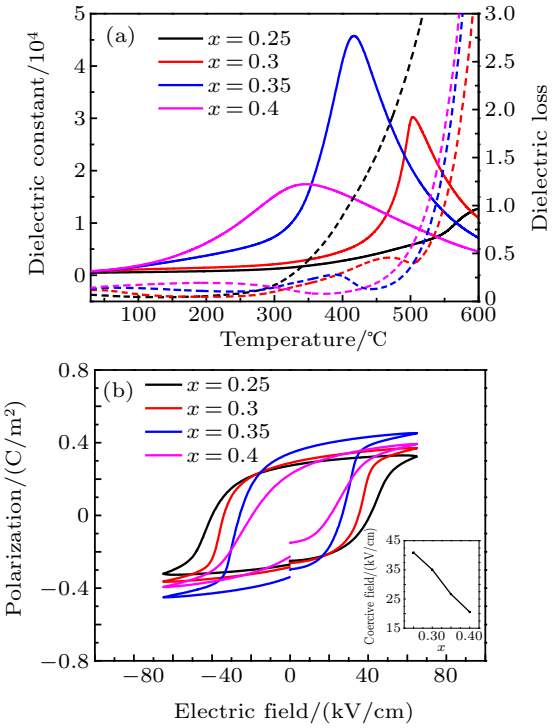


Fig. 2. (a) Temperature-dependent dielectric constants and dielectric losses of $(1-x)$BFO–xBTO ceramic samples (at 100 kHz), and (b) *P*–*E* loops of $(1-x)$BFO–xBTO ceramic samples at room temperature (at 10 Hz), with inset showing coercive field varying with composition quantity.

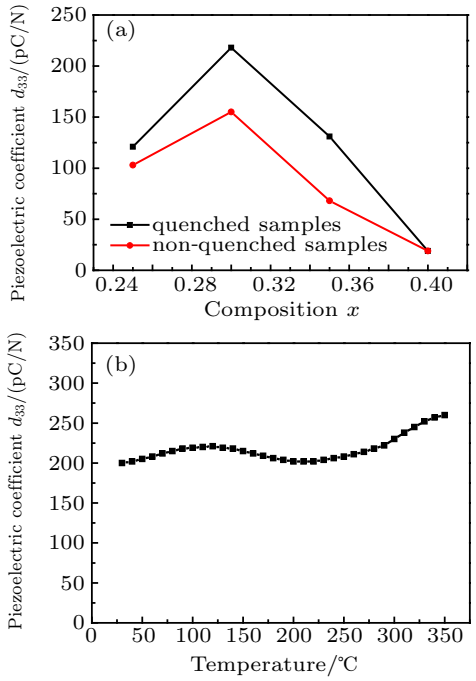


Fig. 3. (a) Piezoelectric coefficient d_{33} *versus* composition of quenched and non-quenched BFO–BTO ceramics, and (b) temperature-dependent d_{33} of quenched 0.7BFO–0.3BTO ceramics from room temperature to 350 °C.

The piezoelectric response is an important parameter for generating the strong ME response. The variations of piezoelectric coefficient d_{33} with composition of the quenched BFO–BTO ceramics are shown in Fig. 3(a). Like the observation in PZT, the maximum d_{33} is measured to be 215 pC/N in

the quenched 0.7BFO–0.3BTO ceramics, a composition near the MPB of the solid solution. In Fig. 3(a), the piezoelectric response of the BFO–BTO ceramics without being subjected to the quenching process is also shown. Consistent with prior studies, the quenching process significantly enhances the piezoelectric response. From Fig. 2(a), we can see that the T_m of 0.7BFO–0.3BTO ceramics with the composition having the highest d_{33} among the BFO–BTO ceramics that we studied (Fig. 3(a)), is ~ 500 °C, which is much higher than the T_c of PZT ceramics. It implies that the piezoelectric response of the ceramics can be sustained at a temperature much higher than that of the PZT ceramics. The temperature-dependent d_{33} of 0.7BFO–0.3BTO ceramics is measured and the result is shown in Fig. 3(b). The d_{33} of the ceramics is slightly dependent on the temperature below 350 °C, suggesting that BFO–BTO ceramics is a class of lead-free piezoelectric material with a high piezoelectric response, which promises to possess high-temperature applications.

Figure 4(a) shows the magnetic hysteresis (M–H) curves for the quenched $(1-x)$BFO–xBTO ceramics with the compositions near the MPB. The changes of magnetization with magnetic field for four different compositions are shown in Fig. 4(a), where the inset displays the residual magnetization and coercove field varying with composition. The remnant magnetization increases first, reaching the maximum value when $x = 0.3$, and decreases then. The variation of magnetic properties with compositions can be attributed to the change of spiral modulated spin structure existing in BFO after incorporating BTO into BFO. The mechanism proposed for the observation of ferromagnetism in BFO–BTO solid solutions was reported in Ref. [16]. We notice that the magnetic properties in the quenched BFO–BTO ceramics are different from those reported in Ref. [16], which can be attributed to the difference in preparation conditions between the studies. Although the magnetic properties of BFO–BTO solid solutions have been widely studied, their magnetic responses in different reports[41–44] seem to be conflicting. Different factors, such as preparation conditions and stress could have a significant effect on magnetic response of BFO–BTO solid solution.[44,45] In our work, it is interesting that the composition is observed to be near the MPB ($x = 0.3$), like other physical properties, such as piezoelectric response, the remnant magnetization reaches a maximum value.

Quenching is found to have a significant effect on the ferromagnetism of the BFO–BTO ceramics. Figure 4(b) shows M–H curves for 0.7BFO–0.3BTO ceramics before and after quenching. An enhanced ferromagnetism is observed in air-quenched sample compared with the sample without being subjected to the quenching process. The remnant magnetization increases from 0.1263 emu/g to 0.2248 emu/g after quenching. The enhancement of ferromagnetism of the quenched BFO–BTO is not clear and needs further studying. Because the stress enhanced ferromagnetism has been observed in BFO-based thin film,[45] we think, the quenching-induced internal stress in the materials could be one mechanism responsible for the enhancement in ferromagnetism of the 0.7BFO–0.3BTO ceramics. The stress may partly destruct the spin cycloid in BFO–BTO, resulting in the enhanced ferromagnetism in the quenched ceramics.

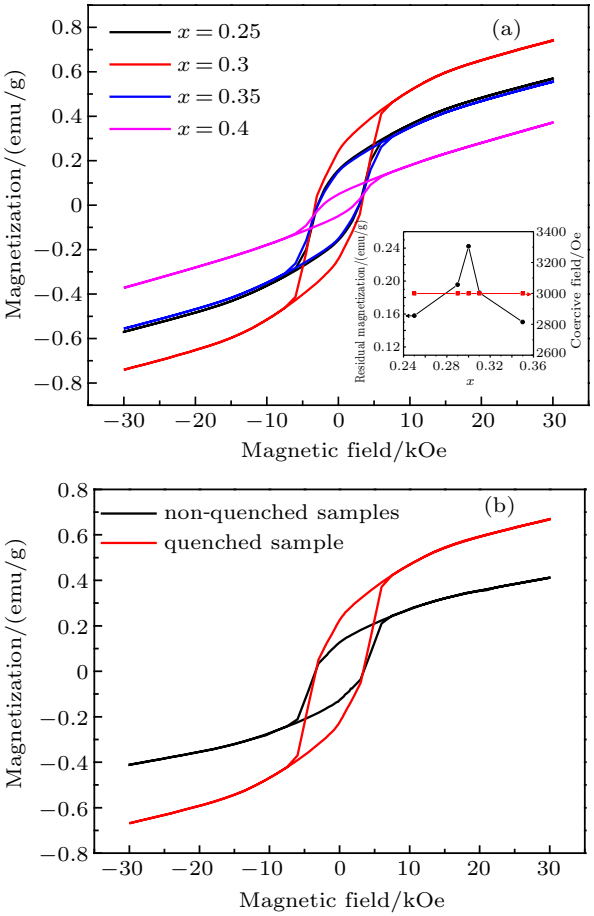


Fig. 4. (a) Magnetic hysteresis curves of quenched $(1-x)$BFO–xBTO ceramics at room temperature for four different compositions, with inset displaying remnant magnetization and coercive field varying with composition of the ceramics. (b) Magnetic hysteresis curve of the quenched and non-quenched 0.7BFO–0.3BTO ceramics at room temperature.

The enhanced piezoelectric and magnetic properties in the quenched BFO–BTO ceramics result in an improved ME response. Figure 5(a) shows the curves of frequency-dependent magnetoelectric coefficient (α_{ME}) of the quenched BFO–BTO rectangular ceramic bars at a DC magnetic field of 6000 Oe. During the ME measurement, the applied magnetic field is parallel to the surface of ceramic bars. As shown in Fig. 5(a), α_{ME} peaks are observed to be in a frequency range between 70 kHz and 100 kHz for these four samples. The peaks are attributed to the excitation of the mechanical resonance in the BFO–BTO ceramics. In the inset of Fig. 5(a), the impedance spectra of 0.75BFO–0.25BTO ceramics are shown, and the resonance and antiresonance peaks originating from the longitudinal mechanical vibration of rectangular

ceramic plates through the transverse piezoelectric response (d_{31}) can be observed. The frequencies for the maximum α_{ME} are consistent with the resonance–antiresonance frequencies measured from the impedance spectra. From Fig. 5(a), it is interesting that the maximum ME response is observed in 0.75BFO–0.25BTO ceramics although the 0.7BFO–0.3BTO ceramics have the largest piezoelectric response (Fig. 3(a)) and the strongest ferromagnetism (Fig. 4(a)), the mechanism of which we will discuss later. A strong ME response $\sim$ 1.3 V/cm·Oe is measured near the resonance frequency of 0.75BFO–0.25BTO ceramic plate. The α_{ME} of 0.6BFO–0.4BTO ceramics is negligibly small compared with those with other compositions because the d_{33} of the composition is small ($\sim$ 19 pC/N, Fig. 3(a)). The plots of dependence of the α_{ME} of BFO–BTO ceramics at non-resonance frequency (10 kHz) on DC magnetic field for four different compositions are shown in Fig. 5(b). The α_{ME} increases linearly with magnetic field increasing and is typically below 0.025 V/cm·Oe. From Figs. 5(a) and 5(b), we can see that the α_{ME} at non-resonance frequency is much smaller than that measured at resonance frequency, reflecting the amplification of the ME response under mechanical resonance conditions.

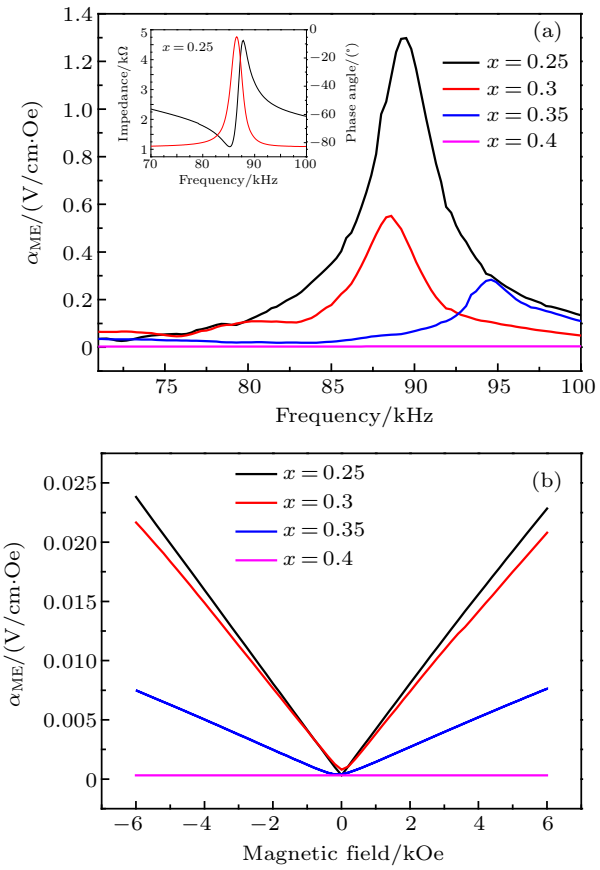


Fig. 5. (a) Frequency-dependent magnetoelectric coupling coefficient α_{ME} measured in $(1-x)$BFO–xBTO ceramics with different compositions under a bias magnetic field of 6000 Oe, with inset displaying impedance spectrum and phase angle spectrum of the 0.75BFO–0.25BTO ceramics with $x = 0.25$. (b) Plots of magnetoelectric coefficient (α_{ME}) *versus* bias magnetic field H_{bias} for $(1-x)$BFO–xBTO ceramic samples with $x = 0.25$, 0.3, 0.35, and 0.4 (measured at 10 kHz).

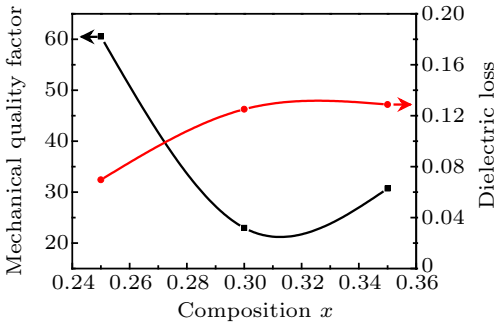


Fig. 6. Mechanical quality factor and dielectric loss *versus* composition of $(1-x)$BFO–xBTO ceramics at room temperature.

Because the ferromagnetism and piezoelectric effect of BFO-based material originate from different microscopic mechanisms, the ME response is generated not from direct coupling of the two physical effects, but through the mechanical interaction. When α_{ME} is measured, the mechanical response is first generated through the magneto-mechanical effect, which, we believe, is the magnetostriction because the sign of α_{ME} does not change after the direction of the applies magnetic DC field has been reversed as shown in Fig. 5(b), and then converted into electrical response by the piezoelectric effect.[46] At mechanical resonance frequencies, the mechanical vibration can be amplified compared with that under the non-resonance state, and a parameter indicating the degree of the amplification is the mechanical quality factor Q_m. The Q_m of the BFO–BTO ceramics near MPB is determined from the impedance spectrum near the resonance–antiresonance frequency, a method that is often used in piezoelectric materials, and the results are shown in Fig. 6. Among the investigated compositions, 0.75BFO–0.25BTO ceramics has the highest Q_m. The Q_m decreases quickly when $x > 0.28$, reaches a minimum value at $x = 0.32$, and then increases slightly when $x = 0.35$. Since the 0.75BFO–0.25BTO ceramics has a much larger Q_m than those of other compositions, it is understandable that the ceramics exhibits the highest α_{ME}. In fact, from Figs. 5 and 6 it follows that the product of the α_{ME} measured at non-resonance frequency and Q_m is roughly equal to the α_{ME} at resonance frequency, indicating that the large α_{ME} of BFO–BTO at resonance frequency is mainly caused by the amplified mechanical vibration at resonance frequency. For example, the α_{ME} of 0.75BFO–0.25BTO ceramics is $\sim$0.024 V/cm·Oe at 10 kHz under a DC magnetic field of 6000 Oe (Fig. 5(b)), and the Q_m is $\sim$ 60 (Fig. 6). The measured α_{ME} at the resonance frequency under the same DC magnetic field is $\sim$ 1.3 V/(cm·Oe), which is close to the product of the α_{ME} at non-resonance frequency and Q_m. In addition to Q_m, which is an indicator of the mechanical loss for mechanical vibration, BFO–BTO ceramics is a dielectric material, and dielectric loss may also be important for the high ME response. Among the investigated compositions, the 0.75BFO–0.25BTO

ceramics has the lowest dielectric loss, which is also desirable for a higher ME response as shown Fig. 6.

4. Conclusions

In this work, $(1-x)$BFO–xBTO ceramics with the compositions near the morphotropic phase boundary is prepared by using a conventional solid-state reaction method and the effect of quenching on the piezoelectric, magnetic, and magnetoelectric properties are investigated. We find that in addition to the piezoelectric response, the quenching of the ceramics from a high temperature can greatly enhance the ferromagnetism of BFO–BTO ceramics. A large piezoelectric response higher than 200 pC/N, which can be sustained at 350 °C, can be achieved in the quenched 0.7BFO–0.3BTO ceramics. Due to the high piezoelectric response and enhanced ferromagnetism of the quenched BFO–BTO ceramics, a greatly enhanced magnetoelectric response up to 1.30 V/cm·Oe is measured in 0.75BFO–0.25BTO ceramics at the mechanical resonance frequency of the sample. The mechanism for the composition dependence of the ME response is also investigated. We show that a high mechanical quality factor and low dielectric loss are desirable to achieve a high ME response, especially under the mechanical resonance conditions.

References

[1] Khomskii D I 2006 *J. Magn. Magn. Mater.* **306** 1
[2] Fiebig M, Lottermoser T, Frohlich D, Goltsev A V and Pisarev R V 2002 *Nature* **419** 818
[3] Ravez J, Abrahams S C and Pape R D 1989 *J. Appl. Phys.* **65** 3987
[4] Sarraute S, Ravez J, VonderMuhll R, Bravic G, Feigelson R S and Abrahams S C 1996 *Acta. Cryst. B.* **52** 72
[5] Ravez J 1997 *J. Phys. III France* **7** 1129
[6] Cheong S W and Mostovoy M 2007 *Nat. Mater.* **6** 13
[7] Palai R, Katiyar R S, Schm H, Tissot P, Clark S J, Robertson J, Redfern S A T, Catalan G and Scott J F 2008 *Phys. Rev. B* **77** 014110
[8] Catalan G and Scott J F 2009 *Adv. Mater.* **21** 2463
[9] Qi X D, Dho J, Tomov R, Blamire M G and MacManus-Driscoll J L 2005 *Appl. Phys. Lett.* **86** 062903
[10] Wang J, Neaton J B and Zheng H 2003 *Science* **299** 1719
[11] Sharma P, Kumar A and Varshney D 2015 *Solid State Commun.* **220** 6
[12] Kumara M and Yadav K L 2007 *Appl. Phys. Lett.* **91** 242901
[13] Lee Y H, Wu J M and Lai C H 2006 *Appl. Phys. Lett.* **88** 042903
[14] Kim J K, Kim S S and Kim W J 2006 *Appl. Phys. Lett.* **88** 132901
[15] Yan T L, Chen B, Liu G, Niu R P, Shang J, Gao S, Xue W H, Jin J, Yang J R and Li R W 2017 *Chin. Phys. B* **26** 067702
[16] Itoh N, Shimura T, Sakamoto W and Yogo T 2007 *Ferroelectrics* **356** 19
[17] Zhang M, Zhang X Y, Qi X W, Li Y, Bao L and GuY H 2017 *Ceram. Int.* **43** 16957
[18] Behera C and Pattanaik A K 2019 *J. Mater. Sci-Mater. El.* **089** 00140
[19] Ryua G H, Hussaina A, Leea M H, Malik R A, Songa T K, KimW J and Kim M H 2018 *J. Eur. Ceram. Soc.* **18** 30341
[20] Du X H, Zheng J H, Belegundu U and Uchino K 1998 *Appl. Phys. Lett.* **72** 2421
[21] Wei Y X,Wang X T, Zhu J T, Wang X L and Jia J J 2013 *J. Am. Ceram. Soc.* **96** 3163
[22] Zhen T, Jiang Z G and Wu J G 2016 *Dalton Trans.* **45** 11277
[23] Lee M H, Kim D J, Park J S, Kim S W, Song T K, Kim M H, Kim W J and Do D 2015 *Adv. Mater.* **27** 6976
[24] He H, Zhao J T, Luo Z L, Yang Y J, Xu H, Hong B, Wang L X, Wang R X and Gao C 2016 *Chin. Phys. Lett.* **33** 67502
[25] Zhao K H, Wang Y H, Shi X L, Liu N and Zhang L W 2015 *Chin. Phys. Lett.* **32** 87503
[26] Rao W, Wang Y B, Wang Y A, Gao J X, Zhou W L and Yu J 2014 *Chin. Phys. Lett.* **31** 017503
[27] Wang Y A, Wang Y B, Rao W, Gao J X, Zhou W L and Yu J 2013 *Chin. Phys. Lett.* **30** 047502
[28] Gupta R, Shah J, Chaudhary S and Kotnala R K 2015 *J. Alloys Compd.* **638** 115
[29] Luo L, Jiang N, Zou X, Shi D, Sun T, Zheng Q, Xu C G, Lam K H and Lin D M 2015 *Phys. Status Solidi A* **212** 2012
[30] Zhang M, Zhang X Y, Qi X W, Zhu H G, Li Y and Gu Y H 2018 *Ceram. Int.* **44** 21269
[31] Bichurin M I, Filippov D A and Petrov V M 2003 *Phys. Rev. B* **68** 132408
[32] Filippov D A, Bichurin M I, Nan C W and Liu J M 2005 *J. Appl. Phys.* **97** 113910
[33] Jia Y M, Luo H S, Zhao X Y and Wang F F 2008 *Adv. Mater.* **20** 4776
[34] Pan Q, Fang C, Luo H S and Chu B J 2019 *J. Eur. Ceram. Soc.* **39** 1057
[35] Pan Q and Chu B J 2019 *J. Appl. Phys.* **125** 154102
[36] *IEEE Standard on Piezoelectricity*, ANSI/IEEE Std. 176-1987, IEEE, New York, 1987
[37] Unruan S, Unruan M, Monnor T, Priya S and Yimnirun R 2015 *J. Am. Ceram. Soc.* **98** 3291
[38] Kumar M M, Srinivas A and Suryanarayana S V 2000 *J. Appl. Phys.* **87** 855
[39] Cao L, Zhou C R, Xu J W, Li Q L, Yuan C L and Chen G H 2016 *Phys. Status Solidi A* **213** 52
[40] Wan Y, Li Y, Li Q, Zhou W, Zheng Q J, Wu X C, Zhu B P and Lin D M 2014 *J. Am. Ceram. Soc.* **97** 1809
[41] Kumar M M, Srinath S, Kumar G S and Suryanarayana S V 1998 *J. Appl. Phys.* **188** 203
[42] Wang T H, Ding Y, Tu C S, Yao Y D, Wu K T, Lin T C, Yu H H, Ku C S and Lee H Y 2011 *J. Appl. Phys.* **109** 07D907
[43] Gotardo R A M, Viana D S F, Olzon-Dionysio M, Souza S D, Garcia D, Eiras J A, Alves M F S, Cotica L F, Santos I A and Coelho A A 2012 *J. Appl. Phys.* **112** 104112
[44] Fujii T, Jinzenji S and Asahara Y 1988 *J. Appl. Phys.* **64** 5434
[45] Bai F M, Wang J L, Wuttig M, Li J F, Wang N G, Pyatakov A P, Zvezdin A K, Cross L E and Viehland D 2005 *Appl. Phys. Lett.* **86** 032511
[46] Ma J, Hu J M, Li Z and Nan C W 2011 *Adv. Mater.* **23** 1062